Nucleic Acids Research, 2005, Vol. 33, No. 22 ***7019–7028***
doi:10.1093/nar/gki1003

Synthesis and hybridization studies of oligonucleotides containing 1-(2-deoxy-2-α-*C*-hydroxymethyl-β-D-ribofuranosyl)thymine (2′-α-hm-dT)

Chang Geng Peng and Masad J. Damha*

Department of Chemistry, McGill University, 801 Sherbrooke Street West, Montreal, QC, Canada H3A 2K6

Received September 8, 2005; Revised and Accepted November 17, 2005

ABSTRACT

We report the first investigation of oligoribonucleotides containing a few 1-(2-deoxy-2-α-*C*-hydroxymethyl-β-D-ribofuranosyl)thymine units (or 2′-hm-dT, abbreviated in this work as 'H'). Both the 2′-*CH$_2$O*-phosphoramidite and 3′-*O*-phosphoramidite derivatives of H were synthesized and incorporated into both 2′,5′-RNA and RNA chains. The hybridization properties of the modified oligonucleotides have been studied via thermal denaturation and circular dichroism studies. While 3′,5′-linked H was shown previously to significantly destabilize *DNA*:RNA hybrids and *DNA*:DNA duplexes (modification in the *DNA* strand; $\Delta T_m \sim -3$°C/insert), we find that 2′,5′-linked H have a smaller effect on *2′,5′-RNA*:RNA and *RNA*:RNA duplexes ($\Delta T_m = -0.3$°C and -1.2°C, respectively). The incorporation of 3′,5′-linked H into *2′,5′-RNA*:RNA and *RNA*:RNA duplexes was found to be more destabilizing (-0.7°C and -3.6°C, respectively). Significantly, however, the 2′,5′-linked H units confer marked stability to RNA hairpins when they are incorporated into a 2′,5′-linked tetraloop structure ($\Delta T_m = +1.5$°C/insert). These results are rationalized in terms of the compact and extended conformations of nucleotides.

INTRODUCTION

Our group has had a long-standing research interest in the physicochemical and biochemical properties of 2′,5′-linked ribonucleic acids (2′,5′-RNA, Figure 1) (1,2). These regioisomers of standard (i.e. 3′,5′-linked) RNA are not only interesting from a structural point of view, but also have potential use in the down-regulation of gene expression (3,4). For instance, 2′,5′-RNAs are able to associate with complementary single-stranded RNA (ssRNA) (3) as well as duplex DNA (5) and, as such, can potentially be used to down-regulate gene expression via the antisense and antigene approaches (Figure 1) (4,6–8). It is also well-documented that annealing two normal RNA strands is more favorable than annealing a 2′,5′-RNA strand with a normal RNA strand (1,3,8,9). Furthermore, mutually complementary 2′,5′-RNA strands have the ability to associate, but exhibit a transition temperature (T_m) that is considerably lower than those of the corresponding RNA:RNA or RNA:2′,5′-RNA duplexes. A comparison of the T_m values of various duplexes of mixed base composition revealed the following order of duplex thermal stability: RNA:RNA > DNA:DNA ≈ DNA:RNA > RNA:2′,5′-RNA > 2′,5′-RNA: 2′,5′-RNA > DNA: 2′,5′-RNA (undetected) (1).

Molecular modeling and circular dichroism (CD) studies of these duplexes revealed that RNA: 2′,5′-RNA hybrids adopt a continuous A-type helix structure similar to that of native RNA (1), but have smaller interstrand phosphate–phosphate distances (by ∼1 Å). This may account, at least in part, for the lower thermal stability of RNA:2′,5′-RNA relative to RNA:RNA and RNA:DNA helices (1).

As part of our ongoing study of these systems, we now present an investigation of 2′,5′-RNA chains containing one or more 1-(2-deoxy-2-α-*C*-hydroxymethyl-β-D-ribofuranosyl)thymine (2′-α-hm-dT; abbreviated in this work as '**H**', Figure 1 and Scheme 1). We anticipated that lengthening the sugar-phosphate backbone by one methylene unit would not only diminish putative P–P repulsions in 2′,5′-RNA:RNA duplexes, but would also provide a 'compact' nucleotide conformation favoring tighter RNA binding (Figure 2) (10,11). This interesting modification was first studied by Schmit *et al*. (12) and reviewed more recently by Freier and Altmann (13). Schmit *et al*. (12) reported that 3′,5′-linked **H** units (3′,5′-**H**) significantly destabilize *DNA*:RNA hybrids and *DNA*:DNA duplexes (modification in the *DNA* strand; $\Delta T_m = -2.9$°C). Destabilization owing to the 2′-α-hydroxymethyl and other

*To whom correspondence should be addressed. Tel: +1 514 398 7552; Fax: +1 514 398 3797; Email: masad.damha@mcgill.ca

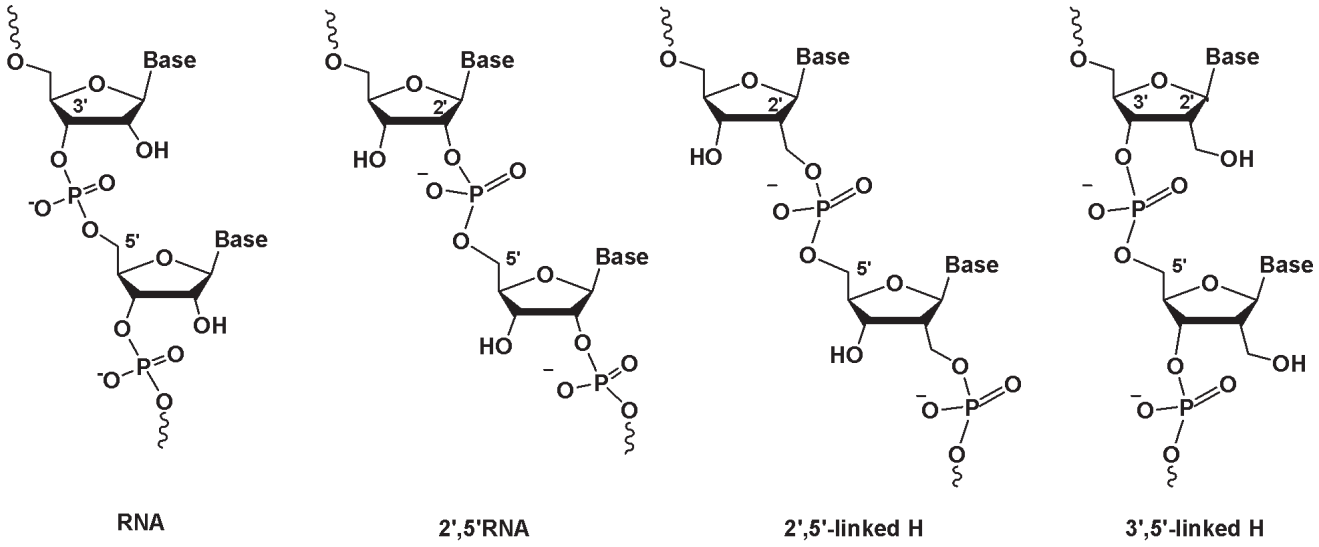

Figure 1. Structure of RNA, 2′,5′-RNA, and strands comprising 2′,5′-linked and 3′,5′-linked **H** units.

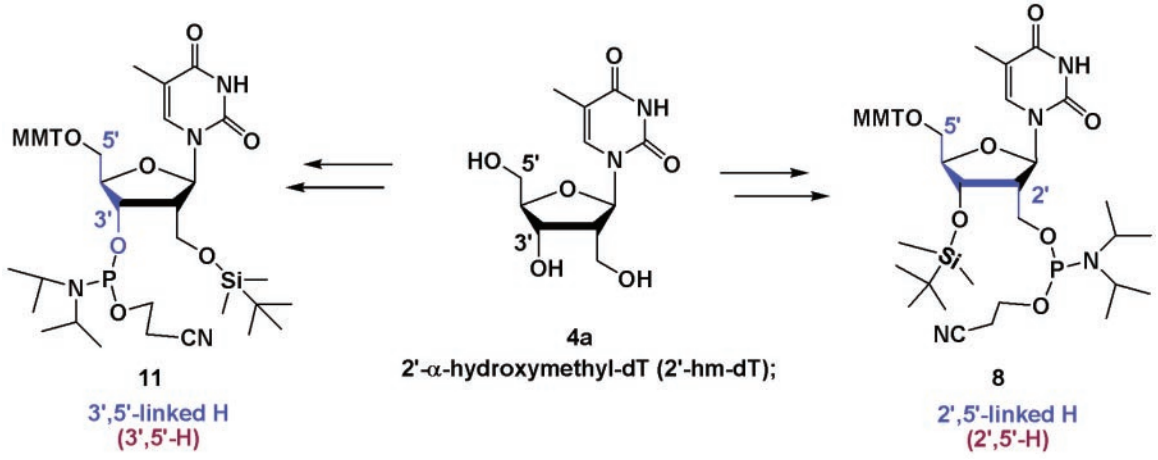

Scheme 1. Structures of 2′-α-hm-dT (**H**) and its phosphoramidite derivatives **8** and **11**.

2′-α alkyl groups was explained by the tendency of these substituents to shift the conformational equilibrium of the sugar toward the C2′-*endo* pucker and away from the C3′-*endo* pucker found in RNA, 2′-*O*-alkyl RNA and 2′F-RNA duplexes (12,13). To the best of our knowledge, neither 2′,5′-linked **H** units (2′,5′-**H**) nor incorporation into RNA have ever been examined. The present study revealed that 2′,5′-**H** units have a modest destabilizing effect on *2′,5′-RNA*:RNA ($\Delta T_m = -0.3°C$) and *RNA*:RNA duplexes ($\Delta T_m = -1.2°C$), whereas 3′,5′-**H** units are significantly more destabilizing ($-0.7°C$ and $-3.6°C$, respectively), consistent with the results of Schmit *et al*. (12). In contrast, we find that 2′,5′-**H** units confer significant stability to RNA hairpins, particularly when they are placed in the loop structure ($\Delta T_m = +1.5°C$).

MATERIALS AND METHODS

General reagents

All reactions were carried out in oven-dried glassware under a N_2 atmosphere. Dichloromethane (CH_2Cl_2) and acetonitrile (CH_3CN) were dried by refluxing and distilling over calcium hydride (CaH_2) under a N_2 atmosphere. Tetrahydrofuran (THF) was dried by refluxing over sodium and benzophenone under a N_2 atmosphere and collected before use. Anhydrous methanol (MeOH), pyridine (py), *N*-ethyl-*N*,*N*-diisopropylamine (DIPEA), *N*,*N*-dimethylformamide (DMF) and 2,6-lutidine were obtained from Aldrich. The following chemicals were used as received from Aldrich: *p*-anisylchlorodipenylmethane (MMTr-Cl), benzoyl chloride (Bz-Cl), *tert*-butyldimethylsilyltriflate (TBDMSOTf), *tert*-butyldimethylsilylchloride (TBDMSCl), 4,5-dicyanoimidazole (DCI), 4-dimethylaminopyridine (DMAP), 1,1,1,3,3,3-hexamethyldisilazane (HMDS), 10 *wt%* palladium on carbon powder (10% Pd/C), triethylamine tris(hydrofluoride) (TREAT HF), *D*-ribose, silver nitrate ($AgNO_3$), 1.0 M tin (IV) tetrachloride solution in dichloromethane ($SnCl_4$), thymine. β-cyanoethyl-*N*,*N*-diisopropylchlorophosphoramidite and other solid-phase synthesis reagents and regular nucleoside monomers were purchased from ChemGenes Corp. (Ashland, MA).

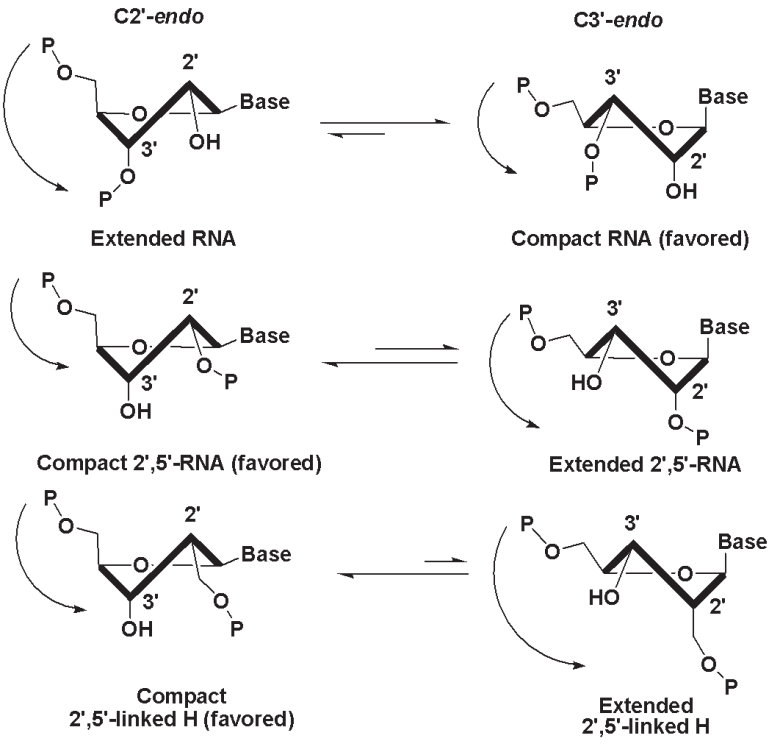

Figure 2. The C2′- and C3′-*endo* sugar puckers are favored in 2′,5′-linked RNA and 3′,5′-linked RNA, respectively (10,11). The intraresidue P–P distance determines the 'compact' or 'extended' backbone structure (11). Lengthening by an extra carbon C2′ (**H**) removes the gauche effect between the ring oxygen and O2′, which is expected to reinforce the C2′-*endo* or compact conformation for 2′,5′-linked **H** units.

Methyl 2-α-benzoyloxymethyl-2-deoxy-3,5-di-*O*-(2,4-dichlorobenzyl)-α-D-ribofuranoside (2)

Compound (**1**) was obtained following slight modifications of the procedure described by Martin [(14); Supplementary Data]. Under a N_2 atmosphere, 1.5 ml (1.78 g, 12.7 mmol) BzCl was added to a solution of **1** (4.83 g, 9.73 mmol) in 75 ml dry pyridine. The resulting solution was kept stirring at room temperature for 4 h. The reaction progress was monitored by TLC. When the reaction was complete, the reaction mixture was concentrated under reduced pressure, and then washed with saturated $NaHCO_3$ and brine. The aqueous phase was extracted with CH_2Cl_2 three times. The combined organic layers were evaporated to dryness to afford **2** in quantitative yield (5.84 g). R_f (SiO_2) = 0.86 (2:1 EtOAc/hexane); 0.70 (1:2 EtOAc/hexane); ^{1}H NMR (400 MHz, $CDCl_3$, δ): 7.98–7.09 (m, 11H, ArH), 5.11 (d, $^3J_{1\text{-}2}$ = 5.2 Hz, 1H, H1), 4.73–4.55 (m, 6H, benzyl CH_2 and CH_2–C2), 4.4–4.43 (m, 1H, H4), 4.08 (dd, $^3J_{3\text{-}2}$, $^3J_{3\text{–}4}$ = 5.2, 2.4 Hz, 1H, H3), 3.54–3.64 (AB dd, $^2J_{5,5'}$ = 22.4 Hz, $^3J_{4,5+5'}$ = 4.4, 5.2 Hz, 2H, H5 and H5′), 3.45 (s, 3H, OCH_3), 2.74–2.67 (m, 1H, H2). ESI-MS for $C_{28}H_{26}Cl_4O_6$ [MNa^+] calcd 621.05, found 621.1.

1-[2-α-Benzoyloxymethyl-2-deoxy-3,5-di-*O*-(2,4-dichlorobenzyl)-D-ribofuranosyl]thymine (3)

Under a N_2 atmosphere, a mixture of dry thymine (1.35 g, 10.7 mmol), ammonium sulfate (0.136 g, 1.029 mmol) and HMDS (2.87 ml, 13.8 mmol) in anhydrous CH_3CN (41 ml) was refluxed at 100°C for 4 h until the reaction mixture was clear. The reaction mixture was cooled to room temperature and added to a solution of **2** (2.47 g, 4.12 mmol) in dry CH_3CN (19.5 ml) followed by 1.0 M $SnCl_4$ in CH_2Cl_2 (4.12 ml, 4.12 mmol). The resulting solution was warmed to 50°C and left stirring for an additional 12 h. After the reaction was complete, the reaction mixture was cooled to room temperature, washed with saturated $NaHCO_3$ (50 ml) and filtered. The filtrate was extracted three times with the same volume of CH_2Cl_2 and the organic layer was washed with brine, dried over Na_2SO_4 and evaporated to yield a white foam. Purification by silica gel column chromatography with EtOAc/hexane (2:1, v/v) afforded the title compound in 72% yield (2.06 g, β:α = 5:1). R_f (SiO_2) = 0.6 (2:1 EtOAc/hexane); ^{1}H NMR of β-isomer (400 MHz, $CDCl_3$, δ): 7.97–7.19 (m, 12H, ArH and H-6), 6.35 (d, $^3J_{1',2'}$ = 8.8 Hz, 1H, H1′), 4.74, 4.47 (2dd, $^2J_{CH2\text{-}C2'}$ = 12 Hz, $^3J_{CH2\text{-}C2',\ H_{2'}}$ = 7.6, 7.2 Hz, 2H, CH_2-C2′), 4.69–4.56 (m, 4H, benzyl CH_2), 4.38 (br, m, 1H, H4′), 4.31–4.28 (m, 1H, H3′), 3.9, 3.7 (2 dd, $^2J_{5',5''}$ = 10.8 Hz, $^3J_{4',5'+5''}$ = 3.2, 2.4 Hz, 2H, H5′ and H5″), 2.99–2.92 (m, 1H, H2′), 1.64 (d, $^4J_{CH3\text{-}C5,H6}$ = 1.2 Hz, 3H, CH_3-C5). ESI-MS for $C_{32}H_{28}Cl_4N_2O_7$ [MNa^+] calcd 717.39, found 717.0.

1-(2-α-*C*-Benzoyloxymethyl-2-deoxy-β-D-ribofuranosyl)thymine (4)

To a solution of **3** (1.065 g, 1.53 mmol) in dry MeOH (50 ml) was added 10% Pd/C (0.39 g, 0.37 mmol). The resulting mixture was kept shaking under 40–50 psi H_2 at room temperature for 6 h. The mixture was filtered and evaporated to dryness, and the residue was purified by silica gel column chromatography (eluent 40:1 to 15:1 CH_2Cl_2/MeOH) to separate the α and β-isomers. The desired β-isomer was obtained in 71% yield (0.41 g). R_f (SiO_2) = 0.51 (6:1 CH_2Cl_2/MeOH); 0.31

(10:1 CH_2Cl_2/MeOH); ^{1}H NMR (400 MHz, DMSO-d_6, δ): 11.22 (s, 1H, N-H), 7.78–7.41 (m, 5H, Bz), 7.7 (s, 1H, H-6), 6.14 (d, $^3J_{1',2'} = 8.8$ Hz, 1H, H1′), 5.52 (d, $^3J_{OH,\ H3'} = 4.8$ Hz, 1H, HO-C3′), 5.1 (t, $^3J_{OH,\ H5'+H5''} = 5.2$ Hz, 1H, HO-C5′), 4.57, 4.26 (2dd, $^2J_{CH2\text{-}C2} = 11.6$ Hz, $^3J_{CH2\text{-}C2,\ H2'} = 5.6, 8.8$ Hz, 2H, CH_2-C2′), 3.88 (br, 1H, H4′), 3.54–3.64 (AB, dd, $^2J_{5',5''} = 17.7$, $^3J_{4',5'+5''} = 5.2, 4.8$ Hz, 2H, H5′ and H5″), 2.72–2.29 (m, 1H, H2′), 1.74 (s, 3H, CH_3-C5). Four NOESY cross peaks identified the β-isomer: H1′-H4′, H2′-H6′, 2′-CH_2-H4′, H5′-H6. ESI-MS for $C_{18}H_{20}N_2O_7$ [MNa^+] calcd 399.13, found 399.1. Isolated α-isomer, ^{1}H NMR (500 MHz, acetone-d_6, δ): 10.11 (s, 1H, N-H), 8.02–7.46 (m, 5H, Bz), 7.9 (s, 1H, H-6), 6.55 (d, $^3J_{1',2'} = 7.5$ Hz, 1H, H1′), 5.13 (d, $^3J_{OH,\ H3'} = 3.5$ Hz, 1H, HO-C3′), 4.66 (m, 1H, H3′), 4.52–4.3 (m, 2H, CH_2-C2′), 4.48 (m, 1H, H4′), 4.19 (br, 1H, HO-C5′), 3.66 (br, 2H, H5′ and H5″), 3.33 (m, 1H, H2′), 1.82 (s, 3H, CH_3-C5). ESI-MS for α $C_{18}H_{20}N_2O_7$ [MNa^+] calcd 399.13, found 399.1.

1-[2-α-*C*-benzoyloxymethyl-2-deoxy-5-*O*-(4-methoxytrityl)-β-D-ribofuranosyl]thymine (5)

Compound **4** (0.555 g, 1.47 mmol) and $AgNO_3$ (0.375 g, 2.21 mmol) were dissolved in dry pyridine (10 ml). The flask was purged with N_2 and a solution of MMTrCl (0.683 g, 2.21 mmol) in dry pyridine (5 ml) was added. After stirring for 6 h at room temperature, the reaction was worked up by evaporating most of the pyridine and taking up the residue in CH_2Cl_2 (20 ml). The solution was washed with saturated $NaHCO_3$ (20 ml), dried, filtered, and finally evaporated to yield the crude product. Purification by silica gel column chromatography with 0.5% NEt_3 in CH_2Cl_2/MeOH (49:1 to 15:1, v/v) afforded the title compound as a white solid (687 mg; 72% yield). R_f (SiO_2) = 0.66 (10:1 CH_2Cl_2/MeOH); ^{1}H NMR (400 MHz, pyridine-d_5, δ): 12.12 (s, 1H, N-H), 6.95–5.75 (m, 19H, ArH), 6.73 (d, $^4J_{CH3\text{-}C5,\ H6} = 1.2$ Hz, 1H, H6), 5.94 (d, $^3J_{1',2'} = 12$ Hz, 1H, H1′), 4.12–3.83 (m, 3H, CH_2-C2′ and H3′), 3.43 (br, m, 1H, H4′), 2.48 (s, 3H, OCH_3), 2.45 (m, 2H, H5′ and H5″), 2.3 (m, 1H, H2′), 0.5 (s, 3H, CH_3-C5). ^{1}H NMR (400MHz, DMSO-d_6, δ): 11.26 (s, 1H, N-H), 7.81–6.88 (m, 19H, ArH), 7.44 (s, 1H, H6), 6.2 (d, $^3J_{1',2'} = 8.8$ Hz, 1H, H1′), 5.62 (d, $^3J_{3',OH} = 5.2$ Hz, 1H, OH), 4.7, 4.31 (2dd, $^2J_{CH2\text{-}C2'} = 11.2$ Hz, $^3J_{CH2\text{-}C2',\ H2'} = 5.2, 8.4$ Hz, 2H, CH_2-C2′), 4.43 (m, 1H, H3′), 4.0 (br m, 1H, H4′), 3.73 (s, 3H, OCH_3), 3.27, 3.16 (2dd, $^2J_{5',5''} = 10.4$ Hz, $^3J_{4',5'+5''} = 6.4, 3.2$ Hz, 2H, H5′ and H5″), 3.01–2.94 (m, 1H, H2′), 1.3 (s, 3H, CH_3-C5). ESI-MS for $C_{38}H_{36}N_2O_8$ [MNa^+] calcd 671.25, found 671.2.

1-[2-α-*C*-benzoyloxymethyl-3-*O*-*tert*-butyldimethylsilyl-2-deoxy-5-*O*-(4-methoxytrityl) -β-D-ribofuranosyl]thymine (6)

To a solution of **5** (205 mg, 0.316 mmol) in dry CH_2Cl_2 was added 2,6-lutidine (0.15 ml, 1.26 mmol) under a N_2 atmosphere. *tert*-Butyldimethysilyl triflate (TBDMOTf; 0.218 ml, 0.948 mmol) was then added dropwise with stirring at room temperature to yield a clear yellow solution. After stirring at 40°C for 12 h, saturated $NaHCO_3$ (12 ml) was added. The aqueous phase was separated and washed several times with CH_2Cl_2. The combined CH_2Cl_2 layers were dried over Na_2SO_4 and evaporated to dryness. Purification by silica gel column chromatography with 0.5% NEt_3 in CH_2Cl_2:MeOH (100:1 to 20:1, v/v) afforded **6** in 72% yield (0.173 g). When the silylation reaction was conducted at room temperature for 4 h, the yield of the title compound increased to 83%. R_f (SiO_2) = 0.64 (15:1 CH_2Cl_2/MeOH); ^{1}H NMR (500 MHz, DMSO-d_6, δ): 11.33 (s, 1H, N-H), 7.83–6.88 (19H, ArH), 7.5 (s, 1H, H6), 6.12 (d, $^3J_{1',2'} = 8.5$ Hz, 1H, H1′), 4.57, 4.3 (2m, 2H, CH_2-C2′), 4.55 (m, 1H, H3′), 3.97 (m, 1H, H4′), 3.71 (s, 3H, OCH_3), 3.24 (m, 2H, H5′ and H5″), 3.0 (m, 1H, H2′), 1.42 (s, 3H, CH_3-C5), 0.8 (s, 9H, *t*-Bu-Si), 0.02, −0.06 (2s, 6H, $(CH_3)_2$-Si). ^{1}H NMR (400 MHz, acetone-d_6, δ): 9.94 (s, 1H, N-H), 7.96–6.91 (17H, ArH), 7.61 (s, 1H, H6), 6.35 (d, $^3J_{1',2'} = 8.8$, 1H, H1′), 4.78–4.42 (m, 3H, H3′ and CH_2-C2′), 4.15 (br, m, 1H, H4′), 3.79 (s, 3H, OCH_3), 3.44 (m, 2H, H5′ and H5″), 3.18 (m, 1H, H2′), 1.44 (s, 3H, CH_3-C5), 0.92 (s, 9H, *t*-Bu-Si), 0.14, −0.08 (2s, 6H, $(CH_3)_2$-Si). ESI-MS for $C_{44}H_{50}N_2O_8Si$ [MNa^+] calcd 785.33, found 758.3.

1-[3-*O*-*tert*-butyldimethylsilyl-2-deoxy-2-α-*C*-hydroxymethyl-5-*O*-(4-methoxytrityl)-β-D-ribofuranosyl]thymine (7)

A saturated solution of NaOMe in MeOH (4 ml) was added to **6** (0.337 g, 0.442 mmol) at room temperature. After stirring for 2–3 h, the reaction mixture was washed with saturated $NaHCO_3$ (10 ml). The aqueous phase was separated and washed several times with CH_2Cl_2. The combined CH_2Cl_2 layers were dried over Na_2SO_4, filtered and evaporated to dryness. Purification by silica gel column chromatography with 0.5% NEt_3 in CH_2Cl_2/MeOH (100:1 to 15:1, v/v) afforded **7** in quantitative yield (290 mg). R_f (SiO_2) = 0.43 (15:1 CH_2Cl_2/MeOH); ^{1}H NMR (400 MHz, DMSO-d_6): δ11.30 (s, 1H, N-H), 7.47 (s, 1H, H6), 7.40–6.89 (m, 14H, ArH), 5.93 (d, $^3J_{1',2'} = 7.6$ Hz, 1H, H1′), 4.57 (d, $^3J_{OH,H3'} =$ 4.8 Hz, 1H, OH); 4.45 (br m, 1H, H3′), 3.90 (br, 1H, H4′), 3.73 (s, 3H, OCH_3), 3.68, 3.45 (2m, 2H, CH_2-C2′), 3.19 (m, 2H, H5′ and H5″); 2.53 (m, 1H, H2′), 1.51 (s, 3H, CH_3-C5), 0.82 (s, 9H, *t*-Bu-Si), 0.05, −0.04 (2s, 6H, $(CH_3)_2$-Si). ESI-MS for $C_{37}H_{46}N_2O_7Si$ [MNa^+] calcd. 681.31, found 681.2.

1-[2-α-*C*-((β-cyanoethyl-*N*,*N*-diisopropylphosphoramidic)-hydroxymethyl)-2-deoxy-5-*O*-(4-methoxytrityl)-β-D-ribofuranosyl] thymine (8)

N-ethyl-*N*,*N*-diisopropylamine (0.276 ml, 0.205 g, 1.58 mmol) was added to a solution of **7** (0.29 g, 0.44 mmol) in dry THF (3 ml) under a nitrogen atmosphere. The reaction was initiated by addition of β-cyanoethyl-*N*,*N*-diisopropylchlorophosphoramidite via syringe (0.125 g, 0.118 ml, 0.528 mmol). After 2 h, the reaction mixture was passed through a 2 cm layer of silica gel (pre-neutralized with 1% NEt_3), and the desired compound eluted by washing with ice cold hexane followed by CH_2Cl_2. Evaporation of the solution afforded the title compound as a nice white foam (353 mg, 97% yield). R_f (SiO_2) = 0.63 (2:1 EtOAc/hexane); ^{31}P NMR (200 MHz, $CDCl_3$, δ): 148.90, 148.24. ESI-MS for $C_{46}H_{63}N_4O_8PSi$ [MNa^+] calcd 881.42, found 881.2.

1-[2-Deoxy-2-α-*C*-hydroxymethyl-5-*O*-(4-methoxytrityl)-β-D-ribofuranosyl]thymine (9)

A saturated solution of NaOMe in MeOH (2 ml) was added to **5** (0.208 g, 0.321 mmol) and the resulting mixture stirred at room temperature for 2 h. The reaction mixture was then washed with brine (5 ml) followed by CH_2Cl_2 (20 ml). The combined CH_2Cl_2 layers were dried over Na_2SO_4, filtered and evaporated to dryness. Purification by silica gel flash column chromatography with 0.5% NEt_3 in CH_2Cl_2/MeOH (15:1, v/v) afforded **9** in quantitative yield (175 mg). R_f (SiO_2) = 0.26 (15:1 CH_2Cl_2/MeOH); ^{1}H NMR (400 MHz, acetone-d_6, δ): 7.6 (d, $^4J_{CH3\text{-}C5,H6}$ = 1.2 Hz, 1H, H6), 7.52–6.91 (m, 14H, ArH), 6.21 (d, $^3J_{1',2'}$ = 8.4 Hz, 1H, H1′), 4.65 (br, m, 1H, H3′), 4.1–4.12 (m, 1H, H4′), 3.98, 3.79 (2dd, $^2J_{CH2\text{-}C2'}$ = 11.2 Hz, $^3J_{CH2\text{-}C2',\ H2'}$ = 10.0, 6.8 Hz, 2H, CH_2-C2′), 3.42–3.35 (AB, dd, $^2J_{5',5''}$ = 9.6 Hz, $^3J_{4',5'+5''}$ = 4.0, 3.2 Hz, 2H, H5′ and H5″), 2.64–2.71 (m, 1H, H2′), 1.49 (s, 3H, CH_3-C5). ^{1}H NMR (500 MHz, DMSO-d_6, δ): 11.3 (s, 1H, N-H); 7.47 (s, 1H, H6); 7.39–6.89 (m, 14H, ArH); 5.97 (d, $^3J_{1',2'}$ = 8.5 Hz, 1H, H1′), 5.3 (d, $^3J_{OH,\ H3'}$ = 5.5 Hz, 1H, 3-OH); 4.54 (bs, 1H, C2′-C-OH); 4.3 (bs, 1H, H3′); 3.91 (m, 1H, H4′); 3.73 (s, 3H, OCH_3); 3.74–3.43 (2m, 2H, CH_2-C2′); 3.2, 3.12 (2dd, $^2J_{5',5''}$ = 10.5 Hz, $^3J_{4',5'+5''}$ = 4.5, 3.0 Hz, 2H, H5′ and H5″), 2.45 (m, 1H, H2′), 1.4 (s, 3H, CH_3-C5); ESI-MS for $C_{31}H_{32}N_2O_7$ [MNa^+] calcd 567.22, found 567.2.

1-[2-α-*C*-*tert*-butyldimethylsilyloxymethyl-2-deoxy-5-*O*-(4-methoxytrityl)-β-D-ribofuranosyl]thymine (10)

To a solution of **9** (0.186 g, 0.342 mmol) in dry pyridine (3 ml) under a N_2 atmosphere was added $AgNO_3$ (0.067 g, 0.393 mmol) followed by TBDMSCl (59 mg, 0.393 mmol). After stirring for 12 h at room temperature, the reaction was concentrated and the residue taken up in CH_2Cl_2. The solution was washed with saturated $NaHCO_3$ (10 ml), dried, filtered, and finally evaporated to yield the crude product. Purification by silica gel column chromatography with 0.5% NEt_3 in CH_2Cl_2/MeOH (100:1 to 15:1, v/v) afforded the title compound in 66% yield (148 mg). R_f (SiO_2) = 0.64 (15:1 CH_2Cl_2/MeOH); ^{1}H NMR (300 MHz, DMSO-d_6, δ): 11.25 (s, 1H, N-H); 7.47 (s, 1H, H6); 7.39–6.87 (m, 14H, ArH); 6.08 (d, $^3J_{1',2'}$ = 8.7 Hz, 1H, H1′); 5.32 (d, $^3J_{OH,\ H\text{-}3'}$ = 4.8 Hz, 1H, OH); 4.31(br m, 1H, H3′); 3.98–3.64 (m, 2H, CH_2-C2′); 3.73 (s, 3H, OCH_3); 3.23, 3.13 (2dd, $^3J_{4',5'+5''}$ = 4.2, 3 Hz, 2H, H5′ and H5″); 2.57 (m, 1H, H2′); 1.37 (s, 3H, CH_3-C5); 0.79 (s, 9H, *t*-Bu-Si); 0.01- -0.04 (t, 6H, $(CH_3)_2$Si); ESI-MS for $C_{37}H_{46}N_2O_7Si$ [MNa^+] calcd 681.31, found 681.2.

1-[2-α-*C*-*tert*-butyldimethylsilyloxymethyl-3-*O*-(β-cyanoethyl-*N*,*N*-diisopropylphosphoramidic)-2-deoxy-5-*O*-(4-methoxytrityl)-β-D-ribofuranosyl]thymine (11)

β-Cyanoethyl-*N*,*N*-diisopropylchlorophosphoramidite (32 µl, 0.034 g, 0.145 mmol) was slowly added to a solution of **10** (0.148 g, 0.121 mmol) and *N*-ethyl-*N*,*N*-diisopropylamine (76 µl, 0.056 g, 0.436 mmol) in dry THF (1.2 ml) under a N_2 atmosphere. After stirring for 2.5 h, the crude mixture was passed through a 2 cm layer of silica gel (pre-neutralized with 1% NEt_3), and the desired compound eluted by washing with ice cold hexane followed by CH_2Cl_2. Evaporation of the solution afforded the title compound as a nice white foam (101 mg, 52% yield). R_f (SiO_2) = 0.46 (2:1 EtOAc/hexane); ^{31}P NMR (200 MHz, $CDCl_3$): δ 151.7, 150.3; ESI-MS for $C_{46}H_{63}N_4O_8PSi$ [MNa^+] calcd 881.42, found 881.2.

Solid-phase synthesis of oligonucleotides

Oligonucleotide syntheses were carried out on a 1 µmol scale using an Applied Biosystems DNA/RNA 381A synthesizer as described previously (1,3,15). Solutions of phosphoramidites **8** and **11** in acetonitrile (0.09 M) were allowed to react with the solid support for an extended coupling time of 30 min using DCI in acetonitrile (0.5M) as catalyst. These conditions afforded >99% coupling efficiency. Deprotection was conducted by addition of (i) conc. aq. ammonia/ethanol (3:1, v/v, 1 ml, 48 h, room temperature) followed by evaporation; (ii) TEA•3HF (100–200 µl, 48 h, room temperature) followed by evaporation. Typically, 40–80 OD units (A_{260}) of the oligonucleotides were obtained at this point. Oligonucleotides were purified by anion-exchange high-performance liquid chromatography (HPLC) (Protein Pak DEAE-5PW column-Waters; 7.5 mm × 7.5 cm), desalted by size-exclusion chromatography on Sephadex G-25 matrix, and characterized by MALDI-TOF mass spectrometry (Kratos Kompact-III instrument; Kratos Analytical Inc., NY). Purity of the isolated oligonucleotides was >95%.

UV thermal denaturation studies

UV thermal denaturation data were obtained on a Varian CARY 1 spectrophotometer equipped with a Peltier temperature controller (Varian, Mulgrave, Australia). Oligomers and complementary targets were mixed in equimolar ratios in 140 mM K^+, 1 mM Mg^{2+} and 5 mM Na_2HPO_4 buffer, pH 7.2, which is representative of intracellular conditions (16). The total strand concentration was 2.6 µM. Samples were heated to 90°C for 5 min, cooled slowly to room temperature, and refrigerated (4°C) overnight before measurements. Prior to the thermal run, samples were degassed by placing them in an ultrasound bath for 1 min. Denaturation curves were acquired at 260 nm at a rate of heating of 0.5°C/min. The data were analyzed with the software provided by Varian Canada and converted to Microsoft Excel. T_m values were calculated as the maximum of the first-derivative plots of absorbance versus temperature and have an uncertainty of ±1°C. Hyperchromicity values (i.e. changes in relative absorbance) were calculated using the formula: $H = (A_t - A_i)/A_h$, where H is the hyperchromicity, A_t is the absorbance at any given temperature (t), A_i is the initial absorbance reading, and A_h is the absorbance at the highest temperature.

Circular dichroism spectra

CD spectra (200–350 nm) were collected on a Jasco J-710 spectropolarimeter at a rate of 100 nm/min using fused quartz cells (Hellma, 165-QS). Measurements were carried out in 140 mM K^+, 1 mM Mg^{2+} and 5 mM Na_2HPO_4 buffer, pH 7.2 (15) at a duplex concentration of 2.6 µM. The temperature was controlled by an external circulating bath (VWR Scientific) at constant temperature (5°C). The data were processed on a PC computer using J-700 Windows software supplied by the manufacturer (JASCO, Inc.). To facilitate comparisons, the CD spectra were background subtracted, smoothed and corrected for concentration so that molar ellipticities could be obtained.

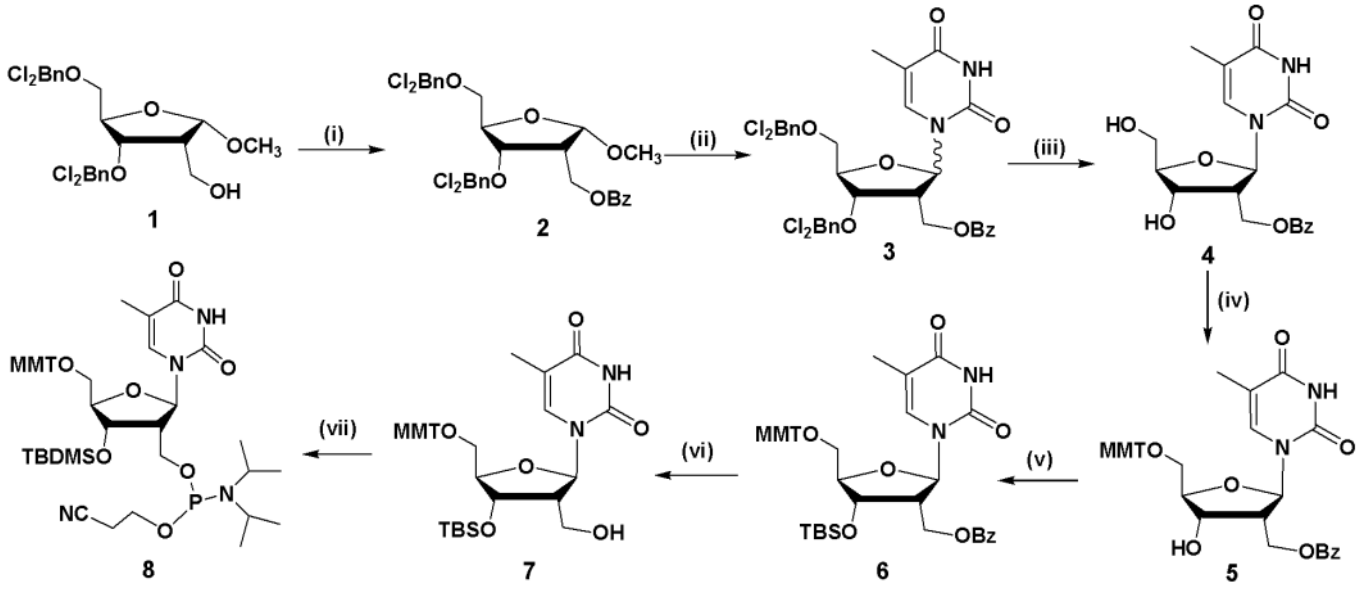

Scheme 2. Synthesis of **8**. (i) BzCl, py., room temperature, 4 h, 100%; (ii) *bis*(trimethylsilyl) thymine, $SnCl_4$, CH_3CN, 50°C, overnight, 72% (isomer mixture, β/α 5:1); (iii) 10% Pd/C, H_2 (40–50 psi), MeOH, room temperature, 6 h, 71% β pure isomer; (iv) MMTr-Cl (1.5 equivalent), $AgNO_3$, py, room temperature, overnight, 72%; (v) TBDMSOTf, 2,6-lutidine, THF, room temperature, 4 h, 83%; (vi) NaOMe, MeOH, room temperature, 2–3 h, 100%; (vii) iPr$_2$NEt, (iPr$_2$N)(OCH$_2$CH$_2$CN)PCl, THF, room temperature, 2 h, 97%.

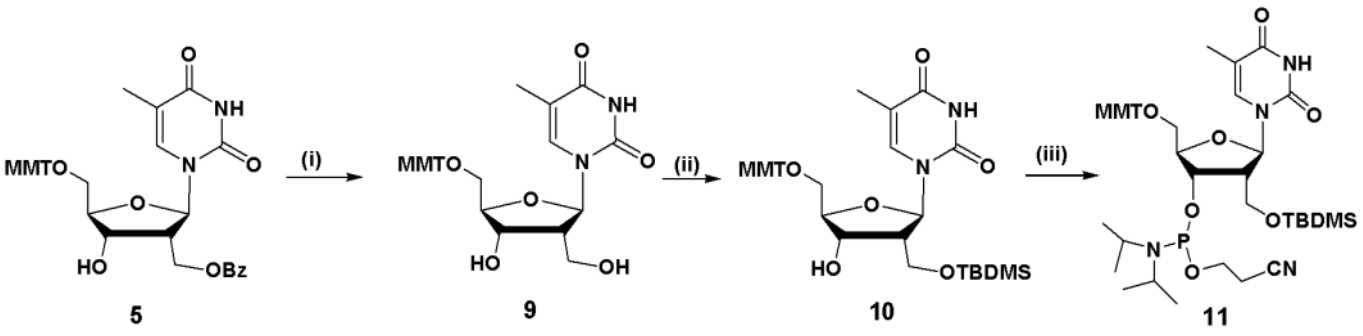

Scheme 3. Synthesis of **11**. (i) NaOMe, MeOH, room temperature, 2 h, 100%; (ii) TBDMSCl, $AgNO_3$, py, room temperature, overnight, 66%; (iii) iPr$_2$NEt, (iPr$_2$N)(OCH$_2$CH$_2$CN)PCl, THF, room temperature, 2.5 h, 52%.

RESULTS AND DISCUSSION

Monomer synthesis

Schemes 2 and 3 show the synthesis of 2′-α-hm-dT (abbreviated in this work as '**H**') and its conversion to the 2′-CH$_2$O- (**8**) and 3′-*O*-phosphoramidites (**11**), using a synthetic strategy analogous to that described previously by Schmit (17) and Li and Piccirilli (18). We protected the C2′-CH$_2$-OH moiety of *O*-glycoside **1** (14) as the benzoyl ester rather than as Schmit's acetyl ester, since we found that the latter was not stable under the conditions of the subsequent hydrogenolysis reaction (Scheme 2). Coupling of **2** with *bis*(trimethylsilyl)thymine in the presence of $SnCl_4$ catalyst gave anomeric nucleosides **3** in good yield with a β/α stereoselectivity of 5:1. It is interesting to note that the β/α stereoselectivity was found to be higher for the C2-CH$_2$-OAc derivative (10:1), in agreement with Schmit's findings (12,17). Separation of the anomers by column chromatography was achieved after removal of the 2,4-dichlorobenzyl protecting groups, to provide the desired β-anomer in 71% yield from **3**. The anomeric configuration of **4** was unequivocally established using NOESY NMR, which displayed strong H1′-H4′, H2′-H6′, 2′-CH$_2$-H4′, and H5′-H6 cross peaks. Reprotection of hydroxyl groups with MMTrCl followed by TBDMSOTf gave **6** in good yields (19). Attempts to carry out the silylation reaction with TBDMSCl (DMF/imidazole or $AgNO_3$/py) proved to be problematic (20). Lastly, we converted **6** to the 2′-CH$_2$O-phosphoramidite derivative **8** via consecutive debenzoylation and phosphitylation reactions (Scheme 2). To access the 3′-*O*-phosphoramidite derivative, nucleoside **5** was treated with NaOMe to give diol **9** quantitatively. Consecutive silylation with TBDMSCl ($AgNO_3$/py) and phosphitylation reactions then afforded the desired compound **11** in moderate yield (52%) (Scheme 3).

Oligonucleotide synthesis

To investigate the effect of 2′,5′- and 3′,5′-linked **H** units on the stability of duplexes, monomers **8** and **11** were incorporated into various oligonucleotide sequences by conventional

Table 1. Thermal denaturation data (T_m) of duplexes

No.	Designation	Oligonucleotide	T_m[a] (ΔT_m)[b] DNA	RNA	2′,5′-RNA
2′,5′-RNA containing 2′,5′-**H** (***H***) and 3′,5′-**H** (**H**)[c]					
I	2,5RNA	5′-rGUC GUG UGU GUG ACU CUG GUA AC-2′	br[d]	61.6	41.3
II	2′,5′-**H**	5′-rGUC UGU ***H***GU GUG CUG GUA AC-2′	br	60.7 (-0.9)	40.5 (−0.8)
III	2′-5′-**H**×2	5′-rGUC UG***H H***GU GUG ACU CUG GUA AC-2′	br	60.6 (-0.5)	40.0 (−0.7)
IV	2′,5′-**H**×3	5′-rGUC UG*H HGH* GUG ACU CUG GUA AC-2′	br	60.5 (-0.3)	39.1 (−0.6)
V	2′,5′-**rA**	5′-rGUC UGU **A**GU GUG ACU CUG GUA AC-2′	br	56.8 (-4.8)	37.3 (−3.5)
VI	2′,5′-r**A** ×2	5′-rGUC UG**A A**GU GUG ACU CUG GUA AC-2′	br	54.3 (-3.7)	34.0 (−3.7)
VII	2′,5′-r**A** ×3	5′-rGUC UG**A A**G**A** GUG ACU CUG GUA AC-2′	br	48.0 (-4.5)	28.0 (−4.3)
VIII	3′,5′-**H**	5′-rGUC UGU **H**GU GUG ACU CUG GUA AC-2′	br	58.0 (-3.6)	37.4 (−3.9)
RNA containing 2′,5′-**H** (***H***) and 3′,5′-**H** (**H**)					
IX	RNA	5′-rGUC UGU UGU GUG ACU CUG GUA AC-3′	65.0	78.4	57.1
X	2′,5′-H	5′-rGUC UGU ***H***GU GUG ACU CUG GUA AC-3′	62.0 (−3.0)	77.2 (−1.2)	52.8 (−4.3)
XI	3′,5′-H	5′-rGUC UGU **H**GU GUG ACU CUG GUA AC-3′	63.0 (−2.0)	77.7 (−0.7)	54.1 (−3.0)
XII	2′,5′-**rU**	5′-rGUC UGU **U**GU GUG ACU CUG GUA AC-3′	62.0 (−3.0)	78.0 (−0.4)	54.1 (−3.0)
XIII	3′,5′-**rA**	5′-rGUC UGU **A**GU GUG ACU CUG GUA ′	61.1 (−3.9)	74.1 (−4.3)	51.1 (−6.0)
DNA control					
XIV	DNA	5′-dGTC TGT TGT GTG ACT CTG GTA AC-3′	68.0	69.0	br

[a]T_m in °C, deviation ±1°C; complementary DNA sequence 5′-dGUU ACC AGA GUC ACA CAA CAG AC-3′; complementary RNA sequence, 5′-rGUU ACC AGA GUC ACA CAA CAG AC-3′; complementary 2′,5′-RNA sequence, 5′-GUU ACC AGA GUC ACA CAA CAG AC-2′; buffer, 140 mM K^+, 1 mM Mg^{2+} and 5 mM Na_2HPO_4, pH = 7.2.
[b]ΔT_m, the T_m change per one modified nucleotide or mismatch relative to entries I or IX.
[c]2′,5′-**H** is shown as ***H***; 3′,5′-**H** as **H**; 2′,5′-r**A** as **A**, 3′,5′-r**A** as **A**; 2′,5′-r**U** as **U** in the sequence.
[d]Broad transition.

phosphoramidite chemistry (Table 1) (1,15,20). 4,5-Dicyanoimidazole (DCI) was used to activate the phosphoramidites (15) and provided average coupling efficiencies of 99% as monitored by the release of the monomethoxytrityl (MMT) cation (Materials and Methods). Deprotection conditions of oligonucleotides were similar to those employed in RNA synthesis (20). Oligonucleotides were purified by anion-exchange HPLC and their identity verified by MALDI-TOF mass spectrometry (Supplementary Data). The HPLC chromatograms showed that 2′,5′-RNA oligomers elute more rapidly relative to 3′,5′-RNA oligomers of the same base composition (Supplementary Data).

Hybridization studies (T_m and CD analysis)

The binding affinity of various mixed backbone oligonucleotides with one to three **H** units to complementary single-stranded DNA (ssDNA), ssRNA and 2′,5′-ssRNA targets was evaluated in a buffer designed to simulate intracellular conditions (Table 1). The oligomers, 23 nt in length, were complementary to portions of the U5 region of HIV-1 genomic RNA. Oligomers containing 2′,5′-**H** substitutions (**II-IV, X**), 3′,5′-**H** substitutions (**VIII, XI**) or mismatched bases (**V-VII, XIII**) were prepared in order to ascertain Watson–Crick pairing of the **H** residues. As a comparison, the hybridization properties of unmodified 2′,5′-RNA (**I**), RNA (**IX**) and DNA (**XIV**) sequences were also measured, along with a 3′,5′-linked oligomer containing a single 2′,5′-linked uridine residue (**XII**). Thermal dissociation data (T_m, ΔT_m) for the complexes formed are presented in Table 1 and representative melting and CD curves are shown in Figure 3. The key observations can be summarized as follows.

2′,5′-H substitutions in the 2′,5′-RNA strand. Both 2′,5′-RNA:RNA and 2′,5′-RNA: 2′,5′-RNA duplexes can accommodate a single 2′,5′-**H** residue with a small loss of stability ($\Delta T_m \sim -0.8$–0.9°C). This destabilization is significantly smaller than that created by a mismatch at the same position ($\Delta T_m \sim -4$°C), suggesting that 2′,5′-**H** residues in these duplexes retain classical base-pairing interactions. When the number of 2′,5′-**H** units is increased to three (e.g. hybrid **IV**:RNA) the depression in T_m is only −0.3°C/modification, suggesting a stabilizing effect by the nearly contiguous 2′,5′-**H** residues (Figure 3A). A nearly superimposable CD signature of the singly and triply substituted hybrids (**II**:RNA and **IV**:RNA) with control duplex **I**:RNA was observed, strongly suggesting that the 2′,5′-**H** inserts do not perturb the global morphology of the duplexes (Figure 3C). The affinity towards RNA targets is likely to be dependent upon the ratio and intrastrand placement of normal (2′,5′-rN) and 2′,5′-**H** units, and based on the above results, a smaller thermal destabilization is to be expected upon increasing the number of consecutive **H** residues. In fact, based on the observed trend from one to three inserts, a fully-modified strand constructed from 2′,5′-**H** units might possibly have a binding affinity to RNA targets comparable with that of 2′,5′-RNA.

The modest destabilization induced by 2′,5′-**H** units is remarkable in view of the one bond chain extension introduced at each of these residues compared with 2′,5′-RNA (Figure 1 and Scheme 1). In addition to the energy (electrostatic) considerations described above, these phenomena may be explained by the anticipated conformation of the 2′,5′-**H** units (Figure 2). Yathindra and coworkers (10,11) have shown that the sugars of 2′,5′-linked RNA favor a C2′-*endo* conformation, which renders the backbone to be 'compact' and of almost equivalent length to that found in the native RNA (i.e. C3′-*endo*). With the C3′-*endo* sugar, the 3′-hydroxyl group would sterically interfere with the 2′-*O*-phosphate linkages. The same 'compact' conformation is expected for 2′,5′-**H** residues, since a strong O4′-C4′-C3′-O3′ gauche effect (and lack of an opposing O4′-C1′-C2′-O2′ gauche effect) would reinforce the C2′-*endo* pucker (Figure 2). Hence, oligonucleotides that are pre-organized in a 'compact' (or RNA-like)

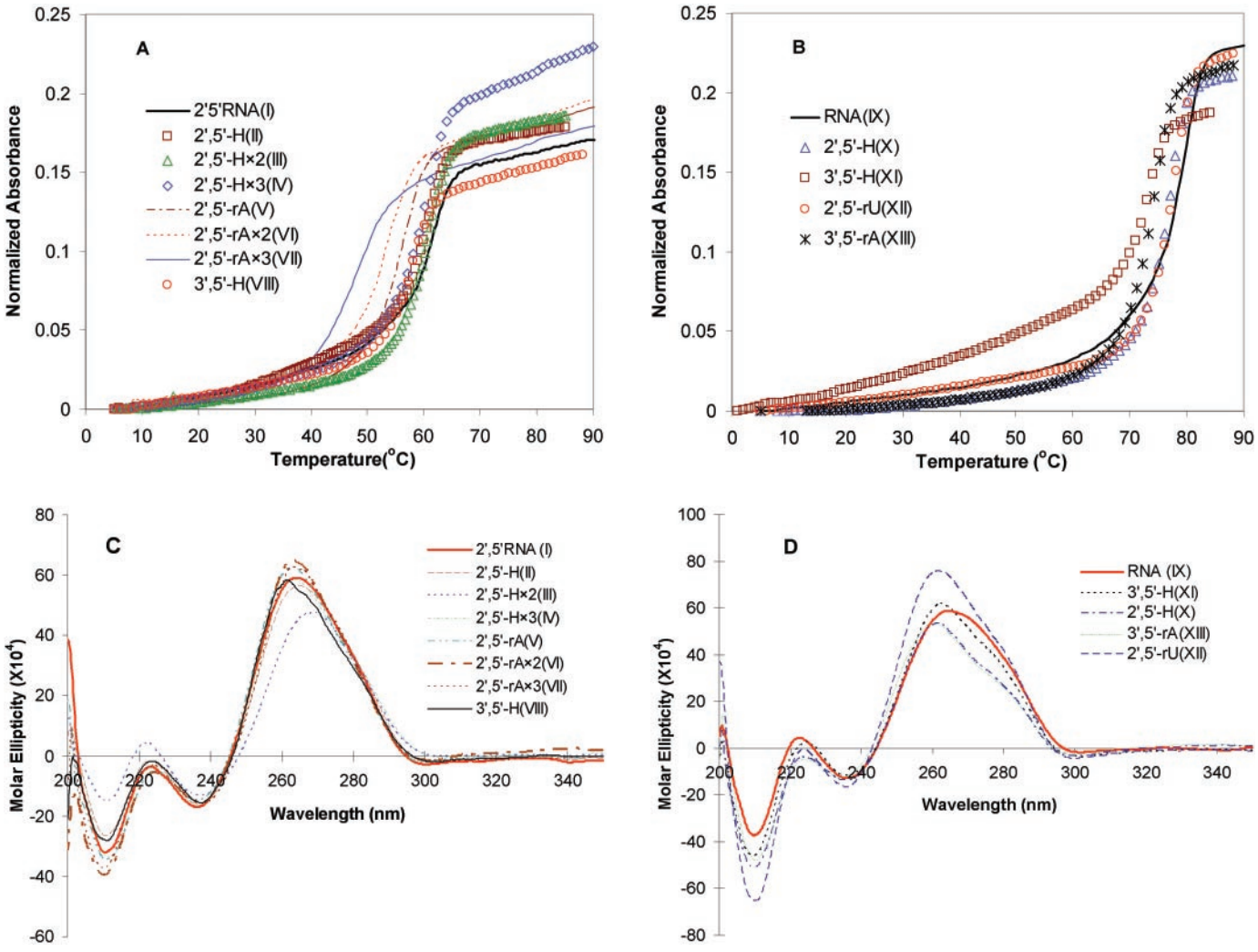

Figure 3. Buffer: 140 mM K^+, 1 mM Mg^{2+} and 5 mM Na_2HPO_4, pH 7.2. Oligonucleotides were hybridized to complementary RNA. (**A** and **C**) Thermal melting curves and CD profile, respectively, of 2′,5′-RNA with 2′,5′-**H**, 3′,5′-**H** and mismatch 2′,5′-rA. (**B** and **D**) Thermal melting curves and CD profile, respectively, of RNA with 2′,5′-**H**, 3′,5′-**H**, 2′,5′-rU and mismatch 3′,5′-rA.

conformation are expected to bind to 'compact' RNA strands, and bind weakly, if at all, to 'extended' oligonucleotide targets (e.g. ssDNA). Such conformational compatibility or spatial 'matching' probably accounts for the ability of oligonucleotides **I** through **VIII** to maintain a stable association with complementary RNA, but not with ssDNA (Table 1) (1).

2′,5′-H substitutions in the RNA strand and 3′,5′-H substitutions in the 2′,5′-RNA strand. The destabilizing effect of 2′,5′-**H** units appears to be greater when incorporated into RNA strands ($\Delta T_m > -1$°C/modification), regardless of whether the target is complementary RNA or 2′,5′-RNA (Sequence **X,** Table 1). Similarly, the presence of 3′,5′-**H** within 2′,5′-RNA leads to reduced duplex stability, with an equal destabilization observed when targeting both RNA and 2′,5′-RNA (Sequence **VIII,** Table 1). Consistent with this notion, the singly-substituted hybrids **VIII**:RNA and **X**:RNA showed a blue shift in the CD band at 270 nm, whereas hybrids **II**:RNA and **XI**:RNA displayed nearly the same CD profile as the corresponding unmodified controls (Figure 3C and D). As pointed out previously (1,11), these observations may reflect the major disruption in the normal helical structure induced by the abrupt displacement of the backbone from the periphery towards the interior of the helix (2′-CH_2OP to 3′-OP) and vice versa (3′-OP to 2′-CH_2OP).

3′,5′-H substitutions in the RNA strand. Regarding the effects of 3′,5′-**H** units within an RNA strand on hybridization affinity for complementary RNA, a significantly less pronounced decrease in duplex stability was observed in *RNA*:RNA duplexes ($\Delta T_m = -0.7$°C) than for Schmit's *DNA*:RNA hybrids (3′,5′-**H** in the antisense DNA strand; $\Delta T_m \sim -3$°C) (12). It may be speculated that this is caused, at least in part, by the narrower minor groove width of *DNA*:RNA hybrids (compared with *RNA*:RNA) leading to more unfavorable interactions involving the large 2′-CH_2-OH group. A much larger decrease in binding affinity was observed for the RNA strand containing a mismatch, confirming the contribution of the thymine base of 3′,5′-**H** to binding (**XIII**:RNA versus **XI**:RNA; Table 1).

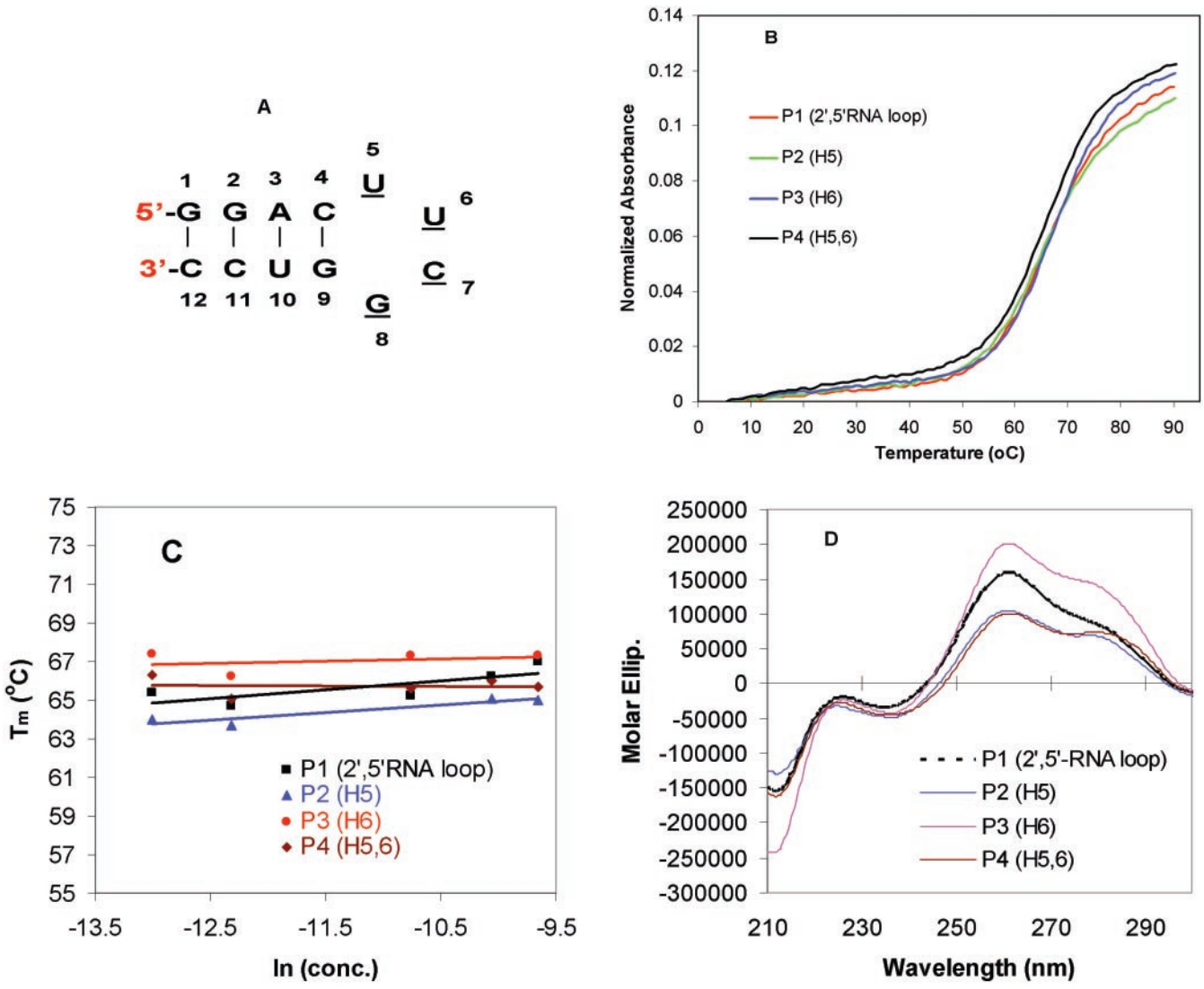

Figure 4. (**A**) Hairpin structure and residue numbering: the tetra loop UUCG is connected via 2′,5′-phosphodiester linkages, and the modification occurs at the U_5 and/or U_6 positions. (**B**) Thermal melting curves of RNA hairpins with modified 2′,5′-linked loops. (**C**) T_m concentration independence over 30-fold range. (**D**) CD spectra.

Stabilization of hairpin structures by 2′,5′-H units

We next turned our attention towards RNA 'hairpins' and studied the effect of incorporating single or multiple 2′,5′-**H** units into the loop of these structures (Figure 4A and Table 2). We have shown previously that hairpin **P1** retains an A-form conformation, displays ample resistance against nucleases, and inhibits the RNase H activity of HIV RT (15,21,22). The ribonucleotide residues in the loop are connected by 2′,5′-phosphodiester linkages and collectively fold into a distinct rigid structure that is unlike the native 3′,5′-tetraloop structure (15). In view of the anticipated compact conformation of 2′,5′-**H** residues (Figure 2), it was of interest to discover how these units would influence the stability of the hairpin. This was particularly intriguing given that a recent study by Denisov *et al*. (22) showed that the 2′,5′-rUCCG loop residues of hairpin **P1** adopt a U5(extended)-U6(compact)-C7(compact)-G8(extended) conformation. Therefore, we anticipated that substitution at position 6 would be better tolerated than one at position 5, particularly if the compact conformation of the 2′,5′-**H** unit was preserved at both loop positions. Indeed, we found that a 2′,5′-**H** unit at position 6 (**P3**) increases hairpin stability, with an increase in T_m of +1.5°C relative to

Table 2. Thermal denaturation data of RNA hairpins with modified 2′,5′-linked loops

ID	Designation[a]	Hairpin loop	T_m[b] (ΔT_m)[c]
P1	RRR	5′-GGAC(UUCG)GUCC-3′	64.7
P2	R$\overline{\text{R}}$(**H**$_5$)R	5′-GGAC($\overline{\textit{H}}$UCG)GUCC-3′	63.7 (−1.0)
P3	RR(**H**$_6$)R	5′-GGAC(U***H***CG)GUCC-3′	66.2 (+1.5)
P4	RR(**H**$_{5,6}$)R	5′-GGAC(***HH***CG)GUCC-3′	65.1 (+0.2)

[a]Underlined residues are connected via 2′,5′-phosphodiester linkages.
[b]T_m was measured at the wavelength of 260 nm in 0.01 M Na_2HPO_4 and 0.1 mM Na_2EDTA, pH 7.0; oligonucleotide concentration ~4.5 μM. Values represent the average of at least five independent measurements. Error in T_m is within ±1°C.
[c]ΔT_m, the T_m change per one 2′,5′-**H**(represented as ***H***in the sequence).

the parent hairpin **P1** (Table 2). This stabilization is nearly offset by the incorporation of a second 2′,5′-**H** unit at position 5 (**P4**, $\Delta T_m = +0.2°C$), which may again be rationalized on the basis of a very strong preference of the 2′,5′-**H** unit for a compact (C2′-*endo*) conformation. In view of this, it is not surprising that a single 2′,5′-**H** substitution at position 5 (**P2**), where an extended nucleotide conformation is preferred, is destabilizing ($\Delta T_m = -1.0°C$). Regarding the CD profiles, the solution conformations of all hairpins are similar to that of the control **P1**, with only slight variations in the intensity of the bands. The hairpins containing 2′,5′-**H** units at position 5 (**P2** and **P4**) were found to present a reduction in the positive CD band at 260 nm (Figure 4D) relative to **P1** and **P3**, consistent with the expected conformational change at this position, i.e. extended 2′,5′-rU→compact 2′,5′-**H**.

CONCLUSIONS

In summary, we have studied the behavior of oligoribonucleotides (2′,5′-RNA and RNA) containing **H** units toward complementary RNA, 2′,5′-RNA and DNA. The data obtained demonstrated a destabilization effect upon substituting a rU with **H**, regardless of whether **H** was 2′,5′ or 3′,5′-linked. This destabilization was minimized when the 2′,5′-**H** and 3′,5′-**H** were incorporated into 2′,5′-RNA and RNA strands, respectively ($\Delta T_m < -1.0°C$). It is expected that longer oligomers containing this modification, particularly if they contain 2′,5′-linkages, will show adequate thermal stability, significant nuclease stability (23) and binding to mRNA targets.

In spite of the drop in thermal stability observed when 2′,5′-**H** units are incorporated into RNA duplexes, a significant increment in stability was observed when they were incorporated into hairpin loops ($\Delta T_m = +1.5°C$). These results and those described above lend strong support to the notion of 'compact'/'extended' 2′,5′/3′,5′-backbone structure and its effect on hybrid stability (11). The ability of hairpins containing stabilizing 2′,5′-**H** units to inhibit HIV RT *in vitro* will be the subject of a separate publication.

SUPPLEMENTARY DATA

Supplementary Data are available at NAR Online.

ACKNOWLEDGEMENTS

We thank Dr R.N. Hannoush for contributions during the early stages of this work. We thank J. Watts, D. Sabatino and M. Mangos for helpful feedback during the preparation of this manuscript. We acknowledge financial support from the Natural Sciences and Engineering Research Council of Canada (NSERC) in the form of a grant to M.J.D. C.G.P. acknowledges support from a FQRNT fellowship and a Clifford Wong McGill Major Fellowship. M.J.D. is recipient of a James McGill Professorship (McGill University). Funding to pay the Open Access publication charges for this article was provided by NSERC Canada.

Conflict of interest statement. None declared.

REFERENCES

1. Wasner,M., Arion,D., Borkow,G., Noronha,A., Uddin,A.H., Parniak,M.A. and Damha,M.J. (1998) Physicochemical and biochemical properties of 2′,5′-linked RNA and 2′,5′-RNA:3′,5′-RNA hybrid Duplexes. *Biochemistry*, **37**, 7478–7486.
2. Peng,C.G., Hannoush,R.N. and Damha,M.J. (2005) Synthesis of a 'taller' 2′,5′-linked ribonucleic acid: 2′-α-C-hydroxymethyl 2′,5′-linked RNA. *J. Biomol. Struct. Dyn.*, **22**, 856.
3. Giannaris,P.A. and Damha,M.J. (1993) Oligoribonucleotides containing 2′,5′-phosphodiester linkages exhibit binding selectivity for 3′,5′-RNA over 3′,5′-ssDNA. *Nucleic Acids Res.*, **21**, 4742–4749.
4. Bhan,P., Bhan,A., Hong,M., Hartwell,J.G., Saunders,J.M. and Hoke,G.D. (1997) 2′,5′-Linked oligo-3′-deoxyribonucleoside phosphorothioate chimeras: thermal stability and antisense inhibition of gene expression. *Nucleic Acids Res.*, **25**, 3310–3317.
5. Damha,M.J. and Noronha,A. (1998) Recognition of nucleic acid double helices by homopyrimidine 2′,5′-linked RNA. *Nucleic Acids Res.*, **26**, 5152–5156.
6. Torrence,P.F., Maitra,R.K., Lesiak,K., Khamnei,S., Zhou,A. and Silverman,R.H. (1993) Targeting RNA for degradation with a (2′-5′)oligoadenylate-antisense chimera. *Proc. Natl Acad. Sci. USA*, **90**, 1300–1304.
7. Xiao,W., Li,G., Maitra,R.K., Maran,A., Silverman,R.H. and Torrence,P.F. (1997) Correlation of selective modifications to a 2′,5′-oligoadenylate-3′,5′-deoxyribonucleotide antisense chimera with affinity for the target nucleic acid and with ability to activate RNAase L. *J. Med. Chem.*, **40**, 1195–1200.
8. Kandimalla,E.R., Manning,A., Zhao,Q., Shaw,D.R., Byrn,R.A., Sasisekharan,V. and Agrawal,S. (1997) Mixed backbone antisense oligonucleotides: design, biochemical and biological properties of oligonucleotides containing 2′-5′-ribo- and 3′-5′-deoxyribonucleotide segments. *Nucleic Acids Res.*, **25**, 370–378.
9. Damha,M.J., Giannaris,P.A. and Khan,N. (1991) 2′-5′-Linked oligonucleotides form stable complexes with complementary RNA and DNA. *Nucleic Acids Symp. Ser.*, 290.
10. Premraj,B.J., Patel,P.K., Kandimalla,E.R., Agrawal,S., Hosur,R.V. and Yathindra,N. (2001) NMR structure of a 2′,5′ RNA favors a type duplex with compact C2′ endo nucleotide repeat. *Biochem. Biophys. Res. Commun.*, **283**, 537–543.
11. Premraj,B.J., Raja,S. and Yathindra,N. (2002) Structural basis for the unusual properties of 2′,5′ nucleic acids and their complexes with RNA and DNA. *Biophys. Chem.*, **95**, 253–272.
12. Schmit,C., Bevierre,M.-O., De Mesmaeker,A. and Altmann,K.-H. (1994) The effects of 2′- and 3′-alkyl substituents on oligonucleotide hybridization and stability. *Bioorg. Med. Chem. Lett.*, **4**, 1969–1974.
13. Freier,S.M. and Altmann,K.H. (1997) The ups and downs of nucleic acid duplex stability: structure-stability studies on chemically-modified DNA:RNA duplexes. *Nucleic Acids Res.*, **25**, 4429–4443.
14. Martin,P. (1995) New access to 2′-*O*-alkylated ribonucleosides and properties of 2′-*O*-alkylated oligoribonucleotides. *Helv. Chim. Acta*, **78**, 486–504.
15. Hannoush,R.N. and Damha,M.J. (2001) Remarkable stability of hairpins containing 2′,5′-linked RNA loops. *J. Am. Chem. Soc.*, **123**, 12368–12374.
16. Alberts,B. (1989) Molecular Biology of the Cell. Carland Publishing, Inc., NY, pp. 304.
17. Schmit,C. (1994) Efficient synthesis of 2′-deoxy-2′-a-C-substituted nucleosides. *Synlett*, 238–240.
18. Li,N.-S. and Piccirilli,J.A. (2004) Synthesis of the phosphoramidite derivatives of 2′-deoxy-2′-C-a-methylcytidine and 2′-deoxy-2′-C-a-hydroxymethylcytidine: analogues for chemical dissection of RNA′s 2′-hydroxyl group. *J. Org. Chem.*, **69**, 4751–4759.
19. Kocienski,P.J. (2004) Protecting group. Georg Thieme, NY, pp. 215.
20. Damha,M.J. and Ogilvie,K.K. (1993) Oligoribonucleotide synthesis. The silyl-phosphoramidite method. *Methods Mol. Biol.*, **20**, 81–114.
21. Hannoush,R.N., Carriero,S., Min,K.-L. and Damha,M.J. (2004) Selective inhibition of HIV-1 reverse transcriptase (HIV-1 RT) RNase H by small RNA hairpins and dumbbells. *ChemBioChem*, **5**, 527–533.
22. Denisov,A.Y., Hannoush,R.N., Gehring,K. and Damha,M.J. (2003) A novel RNA motif based on the structure of unusually stable 2′,5′-linked r(UUCG) loops. *J. Am. Chem. Soc.*, **125**, 11525–11531.
23. Hannoush,R.N., Min,K.-L. and Damha,M.J. (2004) Diversity-oriented solid-phase synthesis and biological evaluation of oligonucleotide hairpins as HIV-1 RT RNase H inhibitors. *Nucleic Acids Res.*, **32**, 6164–6175.